

# GNSS Remote Sensing at GFZ: Overview and Recent Results

Jens Wickert, Galina Dick, Torsten Schmidt, Milad Asgarimehr, Nikolaos Antonoglou, Christina Arras, Andreas Brack, Maorong Ge, Ankur Kepkar, Benjamin Männel, Chinh Nguyen, Temitope Seun Oluwadare, Harald Schuh, Maximilian Semmling, Tzvetan Simeonov, Sibylle Vey, Karina Wilgan and Florian Zus

## Summary

During the recent two decades ground- and satellite-based GNSS remote sensing (GNSS-RS) methods evolved into a versatile and powerful tool for Earth system research on different spatio-temporal scales with operational applications. Large regional and global GNSS ground networks and numerous space-borne receivers provide unique neutral atmospheric/ionospheric data and observations of the Earth's surface. One of the pioneering institutions for these developments is the German Research Centre for Geosciences GFZ at Potsdam. We briefly review recent GFZ developments in GNSS remote sensing.

## Zusammenfassung

In den letzten zwei Jahrzehnten haben sich boden- und satellitengestützte GNSS-Fernerkundungsmethoden zu einem vielseitigen und leistungsfähigen Werkzeug der Erdsystemforschung auf unterschiedlichen raumzeitlichen Skalen mit operationellen Anwendungen entwickelt. Umfangreiche regionale und globale GNSS-Bodennetze und zahlreiche Empfänger auf niedrig fliegenden Satelliten stellen einzigartige Daten der neutralen und ionisierten Atmosphäre und auch Erdoberflächenparameter bereit. Eine der führenden Institutionen bei diesen Entwicklungen ist das Deutsche GeoForschungsZentrum GFZ in Potsdam. Wir stellen ausgewählte aktuelle Forschungsaktivitäten des GFZ in der GNSS-Fernerkundung vor.

**Keywords:** GNSS, Remote Sensing, Atmospheric Sounding, Ionosphere, Reflectometry, Climate Change, Weather Forecast, Space Weather

## Introduction

Backbone of Global Navigation Satellite System (GNSS) Remote Sensing are the GNSS-based techniques for neutral atmosphere/ionosphere sounding, which developed into established tools for Earth observation with numerous operational applications (Elgered and Wickert 2017, Jakowski 2017). Basic principle is the determination of neutral atmospheric/ionospheric parameters (e.g., refractivity, pressure, geopotential height, temperature, water vapor, electron density) based on the observation of GNSS signals propagating in the Earth's atmosphere. Key properties are long-term stability, all-weather capability,

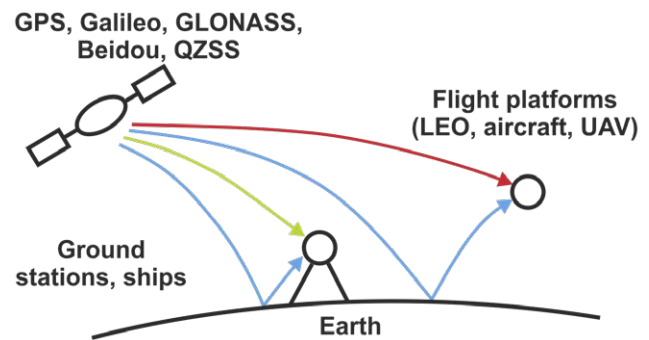


Fig. 1: Observation principle of GNSS remote sensing techniques. Green and red colors indicate ground- and flight platform-based atmosphere sounding. Light blue symbolizes signals, which are reflected from water, ice and land, used to derive geophysical surface parameters.

high accuracy and cost effectiveness. Ground-based techniques allow for a regional monitoring of water vapor and electron density with high temporal resolution (Gendt et al. 2004, Bender et al. 2011). Satellite-based GNSS radio occultation (GNSS-RO) is the basis for the derivation of vertical highly resolved distributions of neutral atmospheric/ionospheric parameters on global scale (Wickert et al. 2009). Therefore, ground- and space-based techniques are complementary to each other with respect to spatio-temporal resolution of the observations. The advantageous properties of the GNSS methods make them appropriate for numerous applications in atmosphere research, improvement of numerical weather forecasts, space weather monitoring and climate research. Hereby the begin of the operational assimilation of ground as well as satellite-based GNSS atmosphere data by several weather centers in 2006 brought the breakthrough for the acceptance of these techniques as established remote sensing methods.

GNSS reflectometry (GNSS-R), i.e., the usage of Earth reflected GNSS signals for remote sensing of ocean, ice and land surfaces was firstly proposed in the early 90s (e.g., Martin-Neira 1993, Hall and Cordey 1988). It is currently in focus of broad international geophysical/geodetic research work (Rius and Cardellach 2017). One main application of GNSS-R is the precise determination of altimetric height and roughness of ocean surfaces. In addition, wind velocity and direction can be derived from the distribution of the backscattered signals (Zavorotny et al. 2014). Another GNSS-R application is the

derivation of the ionospheric propagation delay for correction of altimetric observations from radar satellites. Such data have the potential, e.g., to improve global ionospheric models (Katzberg and Garrison 1996).

The scope of this paper is to give a brief overview on the recent research activities in GNSS remote sensing at the German Research Centre for Geoscience GFZ, which comprises ground-based atmosphere/sounding, radio occultation and reflectometry (Fig. 1).

## 1 Ground-based GNSS atmosphere sounding

### 1.1 Data for operational weather forecast

GNSS meteorology, i.e. ground-based GNSS neutral atmosphere sounding, developed into an established tool for the determination of regional and global atmospheric water vapor distributions on timescales from real-time to cross-decadal for climate change studies. GNSS-derived Zenith Total Delay (ZTD) is currently operationally used to improve numerical weather prediction (NWP) models (e.g. Elgered and Wickert 2017). Next generation data products, such as tropospheric gradient parameters or line-of-sight Slant Total Delays (STDs), are currently in development to be assimilated into NWP models for enhanced forecast capability (e.g. Zus et al. 2019a).

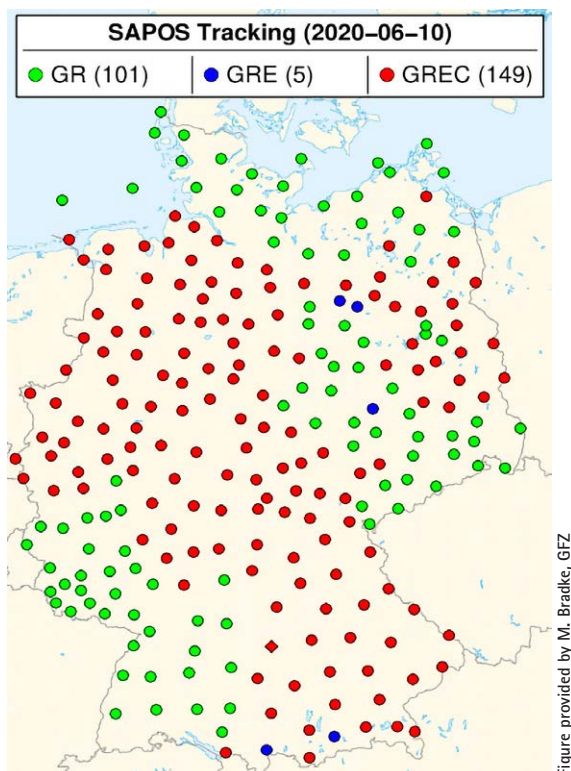


Figure provided by M. Bradke, GFZ

Fig. 2: Availability of Multi-GNSS data from the SAPOS GNSS tracking network in Germany for June 10, 2020. GR (green, 101, GPS and GLONASS); GRE (blue, 5, GPS, GLONASS and Galileo); GREC (red, 149, GPS, GLONASS, Galileo and BeiDou).

GNSS meteorology is an integrative part of the GFZ research activities since 2000. The related scientific work was initiated within the three-year research project GASP (GPS Atmosphere Sounding Project, Reigber et al. 2004). GASP stimulated the operational ground-based GNSS atmosphere sounding using the permanent International GNSS Service (IGS) tracking network, EPN (EUREF Permanent Network) and SAPOS (SATelliten POSitionierungsdienst der deutschen Landesvermessung, see Fig. 2), as well as campaign-type networks, together around 1,300 stations. The data are analysed in near-real time (NRT) for the assimilation to weather models and consistently re-processed for climatological investigations in the framework of the Global Climate Observing System (GCOS). Recent GFZ investigations focus on exploiting the potential of real-time Multi-GNSS observations to improve the atmospheric data products with respect to accuracy, spatio-temporal resolution and latency.

Current standard GNSS data products for the assimilation to numerical weather forecasts are the ZTD and the Integrated Water Vapor (IWV) data above the respective ground stations in near-real time. GFZ contributes significantly to develop advanced data products with improved impact to forecasts in close cooperation with the German Weather Service (Deutscher Wetterdienst, DWD). These products are Multi-GNSS tropospheric gradients (Sect. 1.2.1) and STDs (Sect. 1.2.2). The operational retrieval of STD was established at GFZ for the first time world-wide and they are continuously provided to DWD after intense validation with water vapor radiometer data and other sources. The new assimilation operator for STD was developed at DWD in close cooperation with GFZ.

The GNSS data processing for meteorology is performed with the GFZ Earth Parameter and Orbit determination System (EPOS.P8) software (Dick et al. 2001, Gendt et al. 2004, Ge et al. 2005) which is based on least squares adjustment of undifferenced phase measurements and adheres to IERS Conventions (Petit and Luzum 2010). Operational GNSS data processing at the GFZ is performed in hourly Precise Point Positioning (PPP) mode using 24-hour sliding window approach and provides all tropospheric products: ZTD, IWV, STD and tropospheric gradients in near-real time and in post-processing with 2.5 min (STD) and 15 min (all other products) time resolution.

### 1.2 Development of advanced data products

The development and usage of next generation GNSS-based tropospheric products are in focus of the recent research project AMUSE (Advanced MULTI-GNSS Array for Monitoring Severe Weather Events). It is funded by the DFG (German Research Council) and performed in close cooperation of Technische Universität Berlin (TUB), GFZ and DWD during 2020–2022. AMUSE aims at developments of advanced hourly Multi-GNSS tropospheric

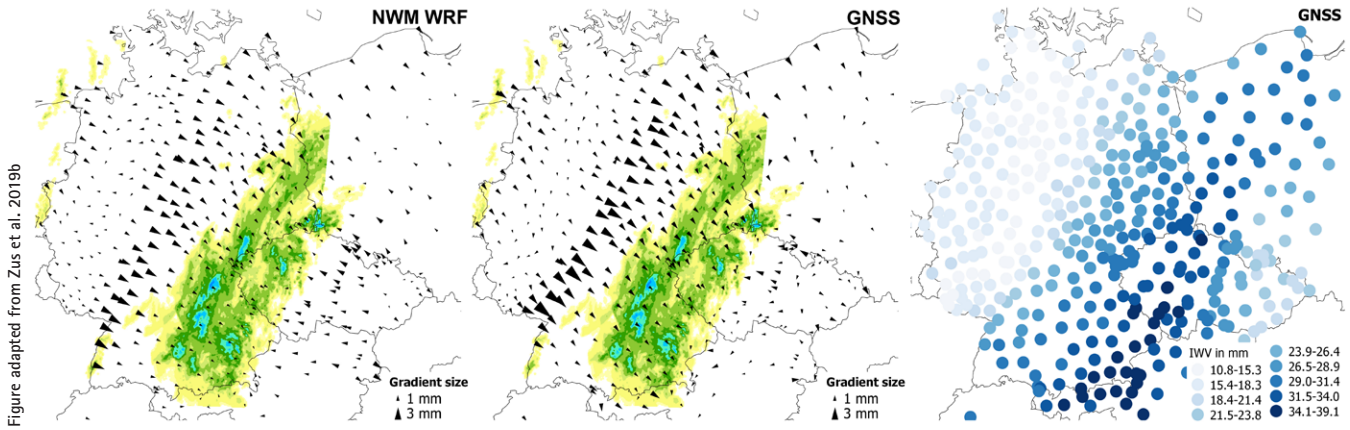


Figure adapted from Zus et al. 2019b

Fig. 3: Meteorological situation on 10 May 2013, at 06:00 UTC, when strong tropospheric gradients are observed. The left panel shows the NWM tropospheric gradient map. The middle panel shows the GNSS tropospheric gradient map. The tropospheric gradient maps are overlaid with radar precipitation provided by the DWD. The radar image shows instantaneous rain in mm/h using a color scale of yellow–green–blue–purple–red, where a darker tone of a specific color means a higher rainfall intensity. The right panel shows the map of Integrated Water Vapor (IWV) data from GNSS.

products, especially gradients and STDs for assimilation into NWP models with the goal to improve the weather forecasts, especially of severe events, in Germany. We briefly introduce the recent work on the tropospheric gradients and STDs in sections 1.2.1 and 1.2.2.

### 1.2.1 Tropospheric gradients

The estimation of tropospheric gradients together with ZTDs (see, e.g., Zus et al. 2019a) is routinely applied in the GNSS data analysis. However, unlike ZTDs which are typically estimated on an hourly basis the tropospheric gradients are typically estimated on daily basis. This is due to the limited observation geometry with a single-system constellation. With the advent of Multi-GNSS (combination of GPS, GLONASS, Galileo, and BeiDou) the observation geometry improves and hence tropospheric gradients are estimated with high temporal resolution (Kačmařík et al. 2019, Li et al. 2015). Fig. 3 shows as an example the GNSS tropospheric gradient map (Germany and Czech Republic) for May 10, 2013, in which large tropospheric gradients are present. For comparison, tropospheric gradients, derived from a Numerical Weather Model (NWM), i.e. the Weather Research and Forecasting (WRF) model (Skamarock et al. 2008) are depicted. In order to show that strong tropospheric gradients are often accompanied by severe weather events, we overlaid the maps with the rain radar image (instantaneous rain) provided by the DWD. We also added the station-specific GNSS IWV values in order to show that the tropospheric gradients can be roughly related to horizontally changing IWV values (IWV gradients). Typically, the tropospheric gradients point from dry to moist areas. Comparisons such as those presented in Fig. 3 triggered the recent studies. For example, the fact that tropospheric gradients can be roughly related to IWV gradients was utilized

in order to show that the IWV interpolation can be improved by utilizing tropospheric gradients (Zus et al. 2019b). Improved IWV fields can be useful for severe weather monitoring. However, it is the (three dimensional) water vapor field that is required in numerical weather prediction. We thus made a first attempt to estimate the impact of tropospheric gradients in variational data assimilation (Zus et al. 2019a).

### 1.2.2 Slant total delays

GFZ provides operationally the STDs from GNSS stations over Germany and the globe (around 500 stations in total). Currently, the GPS-only STDs are calculated using EPOS.P8 and are provided hourly with latency of 25 min. In the AMUSE project, the objective is to calculate Multi-GNSS STDs with a shorter latency of only 15 min ('ultra-rapid' processing). The new products will be operationally assimilated by DWD. The GNSS STDs are compared to STDs calculated from the atmospheric reanalysis ERA5 (Zus et al. 2014). Fig. 4 shows the differences between GNSS and ERA5 derived STDs for all

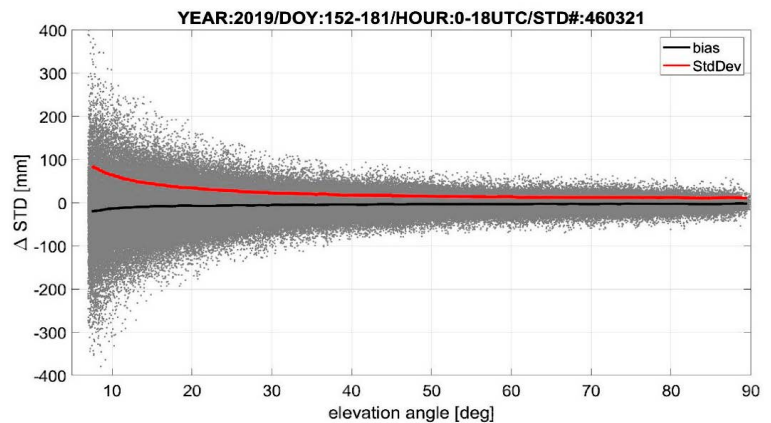


Fig. 4: The difference between GNSS and ERA5 STDs as a function of the elevation angle. The black line indicates the mean deviation and the red line indicates the standard deviation.

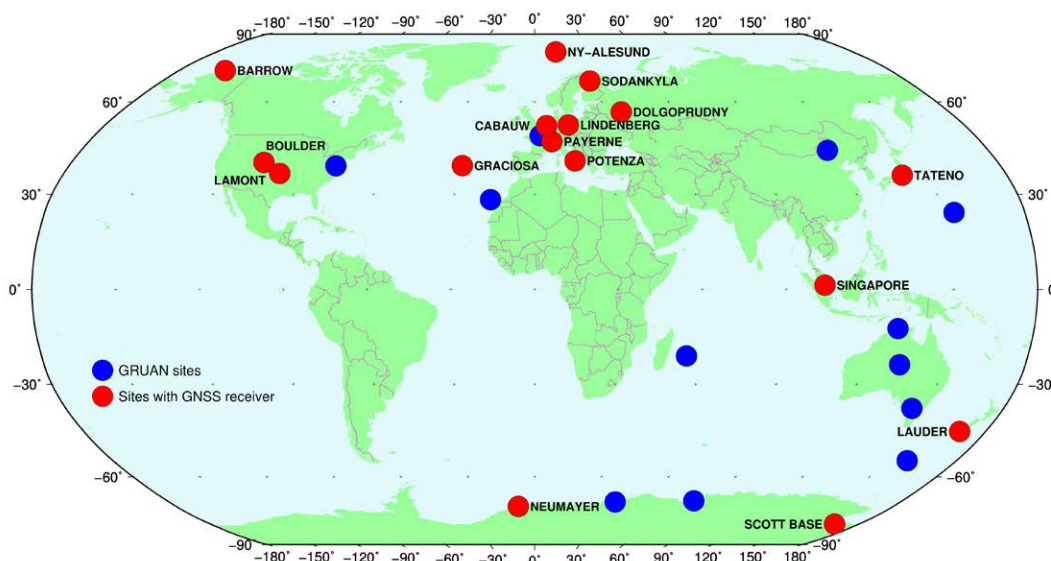


Fig. 5: Current status of the GRUAN network (blue + red stations). As of June 2020, it consists of 28 stations, 16 of them (red) are equipped with GNSS sensors for water vapor determination.

500 stations for June 2019. As the STD values depend on the signal path, larger values and, therefore, higher differences between GNSS and ERA5 related STDs are expected for low elevations. Although, taking the relative differences into consideration, the bias is equal to  $-0.1\%$  with  $0.5\%$  standard deviation averaged over all stations, dates and elevation angles.

### 1.3 Climate monitoring using GNSS

The Global Climate Observing System (GCOS) Reference Upper Air Network (GRUAN) of the World Meteorological Organization (WMO) is an international reference observing network (Fig. 5), designed to meet climate requirements and to fill a major gap in the current global observing system. Upper air observations within the GRUAN network provide long-term high-quality data for the reliable determination of climatological trends to enable deeper understanding of atmospheric processes (e.g., Rinke et al. 2019). GRUAN is envisaged as a global network of 30 to 40 stations with a GNSS receiver as key equipment for water vapor determination. Precise GNSS data analysis is a precondition to get highest level of data quality to fulfill the observation requirements for climate research (e.g., Ning et al. 2016a). GFZ is member of the GRUAN GNSS task team, which defines and controls the observation standards (e.g., Ning et al. 2016b). GFZ also contributes to the GNSS station hardware (Ramatschi et al. 2019) and was selected as the central GRUAN GNSS data processing center. Since 2013 the related automated processing system has been established with the EPOS.P8 software (see Sect. 1.1). An algorithm for the uncertainty estimation of the IWV products has been developed by Ning et al. (2016b). Presently, GFZ generates IWV products including the uncertainty estimation for 13 GNSS stations within GRUAN (Fig. 5). A comparison of GRUAN GNSS data products (GPS-based only) with radiosonde and data from the atmospheric

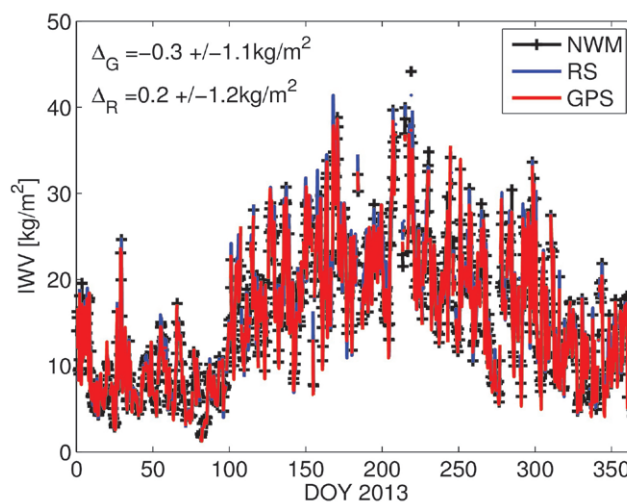


Fig. 6: GPS-derived Integrated Water Vapor (IWV) in 2013 for the GRUAN station Lindenberg (GRUAN product). Data from the co-located radiosonde (RS) and the atmospheric reanalysis model ERA5 (NWM) are shown for comparison.  $\Delta_G$  and  $\Delta_R$  indicate the deviations from ERA5 to GPS (G) and radiosondes (R), respectively. Six-hourly GNSS data and model data, synchronized with the radiosonde measurements, are the basis for this comparison.

reanalysis model ERA5 for 2013 is shown in Fig. 6 (station Lindenberg, Germany).

### 1.4 Global ionospheric maps

GNSS is an effective tool to monitor the Earth's ionosphere by measuring its Total Electron Content (slant TEC) along the signal paths from the navigation satellites to the ground receivers. Such data can be used not only for ionosphere studies, but also to improve the quality of GNSS data products in general. One example is the application of global TEC maps to correct for second order ionospheric delays in the operational generation of GFZ orbit, clock, and troposphere products.

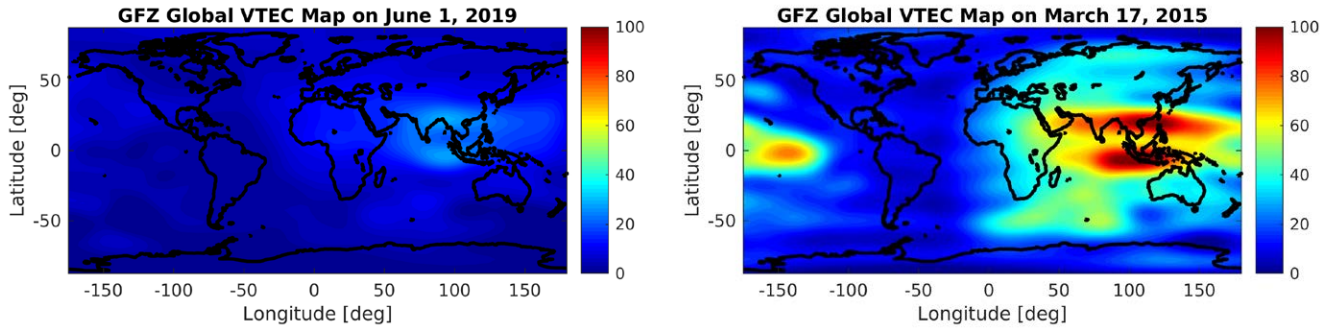


Fig. 7: Global ionospheric maps showing the VTEC in TEC units during a day with moderate ionospheric activity (left) and during the St Patrick's Day geomagnetic storm (right).

A continuous spatiotemporal representation of the vertical TEC (VTEC) is obtained by fitting the GNSS derived slant TEC values from a global reference network to an ionospheric background model. In our processing with the GFZ EPOS.P8 software we currently use ~250 globally distributed stations and a spherical harmonic model representation. Fig. 7 shows exemplarily two maps with moderate and high ionospheric activity. Annual and seasonal variations of the global mean VTEC, derived from such maps, as well as the signature of the solar-cycle, can be seen in Fig. 8. The GNSS derived values strongly resemble the characteristics of the solar flux.

### 1.5 Ionospheric scintillation monitoring

Rapid fluctuation of the amplitude-phase of radio signals, caused by small-scale structures in the ionosphere (ionospheric scintillation), is one of the most unpredictable error sources for nearly all GNSS applications. To monitor it on global scale, we use the ROTI (Rate of TEC Index, Pi et al. 1997). Compared to the traditional method of determining scintillation, that is using the S4 index, directly derived from the high-rate GNSS receivers (usually 50 Hz), this method only needs to use data of conventional dual-frequency receivers. Fig. 9 shows exemplarily a global ROTI map for March 26, 2015, directly

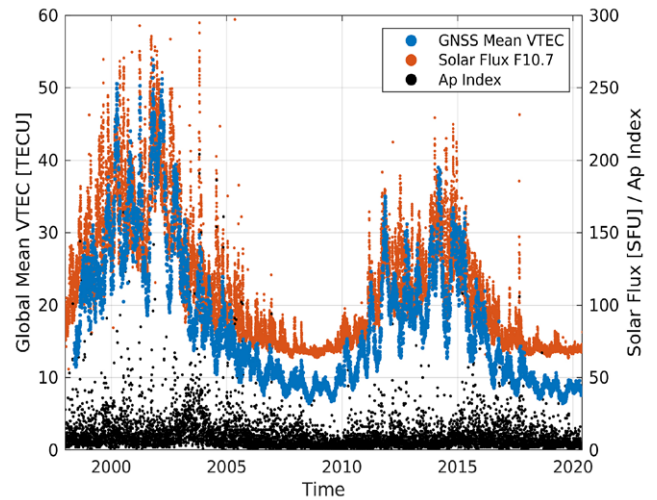


Fig. 8: Time series of the GNSS-derived global mean VTEC values using the IGS ionospheric maps (Hernández-Pajares et al. 2009), of the solar flux F10.7 index, and of the Ap geomagnetic index\*.

\* The solar flux and Ap data are provided by the National Research Council of Canada and GFZ.

after St Patrick's geomagnetic storm (March 17–21, 2015). GNSS data (30 s resolution) from 483 IGS stations were used for this plot. Regions, mostly affected by the ionospheric disturbances are South America, Southeast Asia, and the Arctic. The results for five different latitude

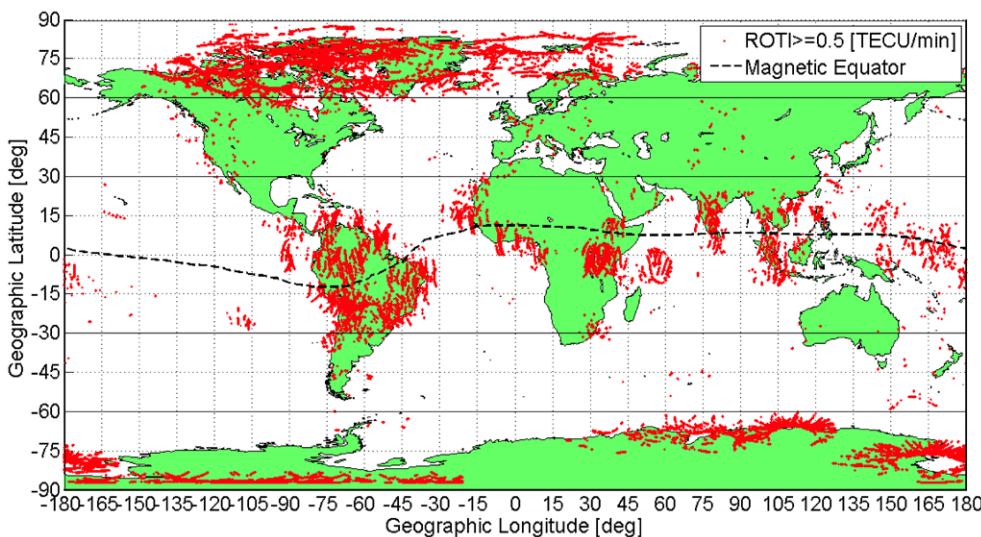


Fig. 9: Spatial distribution of global ionospheric irregularities, based on the Rate of TEC index for March 26, 2015 (only ROTI  $\geq 0.5$  TECU/min are displayed). The plot is based on data from 483 IGS stations.

regions (see Fig. 9) indicate, that the irregularities mainly occur at low latitudes (45.7 % of detected irregularities), followed by the north and south polar regions (32.4 % and 18.3 %, respectively). Also the temporal distribution on March 26, 2015, has a clear latitude dependency. At low latitudes about 97.0 % of the irregularities appeared during the nighttime from 19:00 LT to 02:00 LT the next day. This is in contrast to the polar areas, where scintillations can occur at any time of the day.

### 1.6 Travelling ionospheric disturbances

Travelling Ionospheric Disturbances (TIDs) are signatures in the ionosphere induced by atmospheric gravity waves (AGWs), originated from the troposphere (Jonah et al. 2016). TIDs are capable of producing ionospheric disturbances, that can degrade communication and navigation signals (Hernández-Pajares et al. 2006). Fig. 10 shows – exemplarily for our related investigations to characterize TID distribution – a first-time regional view of TIDs distribution by amplitude (Amp) over Africa. The following values were obtained: 163.7–218 m/s, 26.5–29.4 min, and 149–190 km for TIDs propagation speed, occurrence period, and wavelength, respectively. These values characterize medium-scale TIDs (MSTIDs). The MSTIDs seem to propagate towards the geographic and geomagnetic equator during the post-sunset hours, but more dominant around the geographic equator.

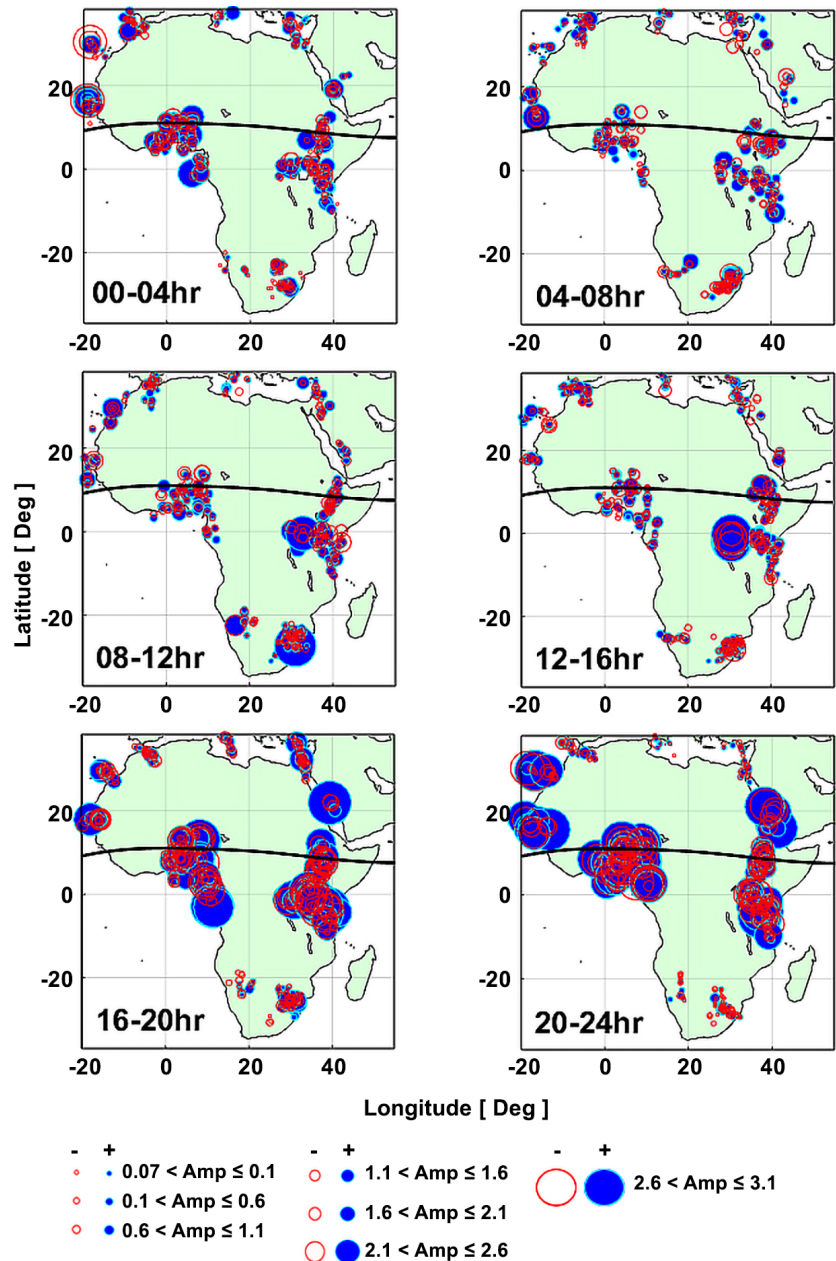


Fig. 10: MSTIDs amplitude regional distributions at four-hour intervals during September 21, 2011. The blue circles indicate a positive amplitude (Amp), while the red empty circles indicate a negative amplitude. The size of the circles indicates the variability of TEC perturbation ( $\sim \pm 3$  dTEC).

## 2 Space-based atmosphere sounding: GNSS radio occultation

### 2.1 Operational data analysis

Within the recent two decades, GNSS-RO has been established as an excellent method for global and continuous monitoring of the Earth's atmosphere (Elgered and Wickert 2017). All leading weather centres assimilate RO data into their forecasts, mainly due to their high impact compared to other observation techniques (e. g., Cardinali and Healy 2014).

The operational use of RO data as, e. g., vertical bending angle or refractivity profiles, by the weather centers, requires appropriate product provision within time limits of around three hours between measurement and data provision. Several automated processing systems, operated by the RO analysis centers for various missions, currently provide such data. GFZ started to develop such NRT system as a part of the CHAMP mission (2001–2008; Schmidt et al. 2005, Wickert et al. 2001). It was extended to the data from GRACE (2006–2017), TerraSAR-X (since 2008), and Tandem-X (since 2011). GRACE-FO (launched mid 2018) data are currently prepared to be processed

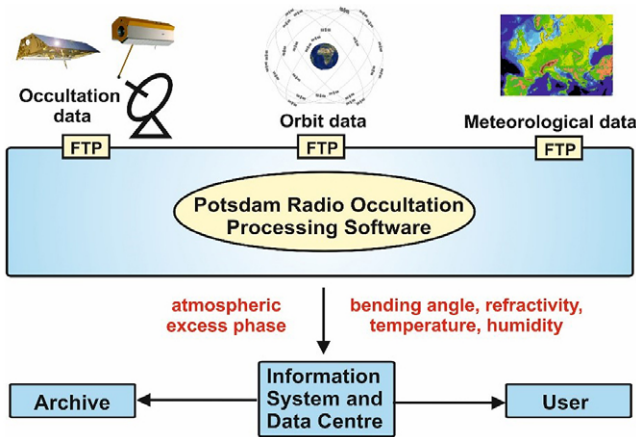


Fig. 11: Infrastructure and data flow of the Potsdam Radio Occultation Processing Software (PROPS) at GFZ. Currently RO data from TerraSAR-X, TanDEM-X are processed operationally to provide products for the international weather services.

by the revised operational GFZ analysis software PROPS (Potsdam Radio Occultation Software, Fig. 11).

The software runs in two different processing modes: NRT and standard. The daily averaged time delay between RO measurements aboard the satellites and availability of the corresponding NRT analysis results via the Global Telecommunication System (GTS) is currently less than 1.5 hours for ~50 % and less than three hours for ~90 % of the products (Fig. 12). Quality checked profiles of atmospheric parameters are available on demand based on the post-processing (standard) mode. These data sets serve for climate and other atmospheric studies (e.g., Schmidt et al. 2016, 2010).

The realization of PROPS follows the principle of separating the processing system into a scientific and controlling part leading to an independent and more flexible software development. The PROPS software is designed to be easily extendable by additional scientific modules or input data. Thus, it also allows for an extension to other single- or multi-satellite radio occultation missions, as e.g., COSMIC/COSMIC-2 or Metop.

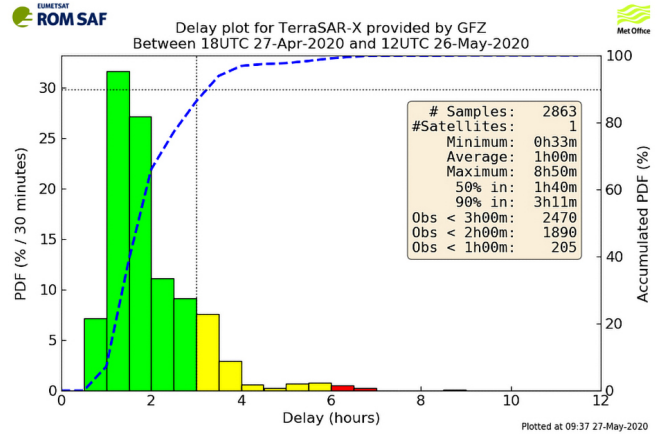


Fig. 12: Example (April/May 2020) of time delay between onboard measurements and provision of corresponding operational GFZ data products for TerraSAR-X (Monitoring by ROMSAF/EUMETSAT, www.romsaf.org). 86 % of the profiles are provided with delay of less than three hours.

## 2.2 Global morphology of ionospheric sporadic E layers

GPS radio occultation enables the global detection and observation of sporadic E layers (Arras et al. 2008, Arras 2010). The electron density enhancements appear in the E region of Earth's ionosphere at an altitude of about 90 to 120 km above the surface. Their formation is controlled by complex ionosphere-neutral atmosphere coupling processes. Sporadic E layer occurrence can be identified using the Signal-to-Noise Ratio (SNR) profiles of the GPS L1 occultation observations. In some cases, the profiles include strong fluctuations at the E region altitude that are caused by strong vertical electron density gradients which can be associated with sporadic E layers (Arras et al. 2010, Wickert et al. 2004). Analyzing about seven million available RO profiles from FormoSAT-3/COSMIC, we received a comprehensive picture of global sporadic E occurrence. As visible in Fig. 13, sporadic E rates enhance strongly at mid latitudes of the actual summer hemisphere.

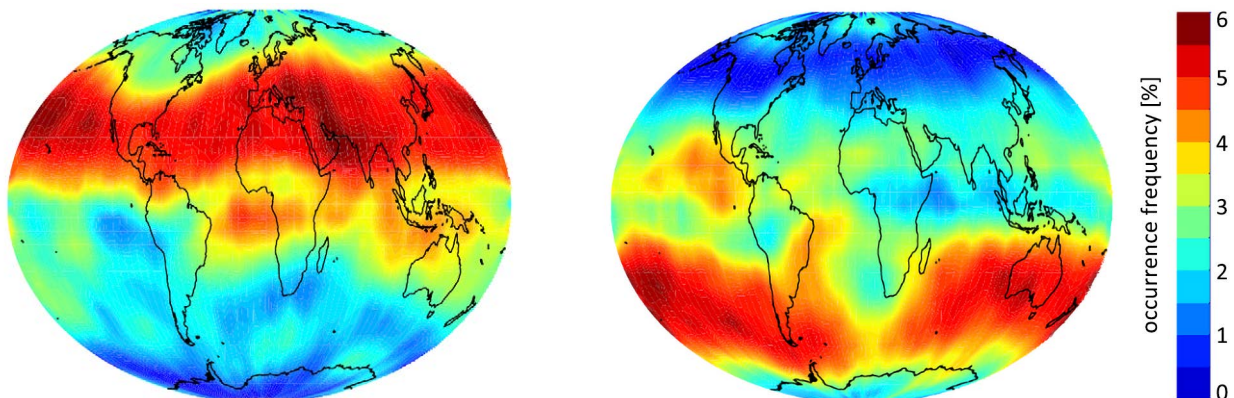


Fig. 13: Global maps of sporadic E occurrence, constructed from GPS radio occultation measurements by FormoSAT-3/COSMIC. The plots include data from the years 2013 and 2014 for northern hemispheric summer (left) and winter (right) conditions.

In contrast, they are very low on the winter hemisphere, in polar regions, and directly along the magnetic equator.

### 2.3 Occurrence climatology of equatorial plasma bubbles

Another global ionospheric RO application are studies of scintillations in the low latitude F-region, i.e., Equatorial Plasma Bubbles (EPBs). A plasma bubble generally occurs during the night and consists of small-scale irregularities that induce fluctuations in the amplitude as well as phase of the radio signals. Previous studies of the plasma bubbles, which were restricted either to a landmass using ground-based instruments or height using in-situ measurements could now be studied globally as well as vertically employing high resolution radio occultation measurements.

EPBs are classified based on the amplitude scintillation index that is derived from 1 Hz signal-to-noise ratio profiles. These profiles are extracted within the altitude range between 150 km and 600 km, thereby excluding the noise from the lower and higher ionosphere. Fig. 14 provides global occurrence maps of EPBs, derived from FormoSAT-3/COSMIC radio occultation measurements. EPBs follow the course of the geomagnetic equator during high and low solar activity, thus providing general evidence on the periodical dependence on the solar cycle. It also appears, that the occurrence peak is shifted between the American and African sectors depending on different solar conditions due to electrodynamics of the ionosphere which is briefly described by Kepkar et al. (2020) along with occurrence dependence of EPBs on longitudes, seasons and altitude.

## 3 Earth surface observation: GNSS reflectometry

The main motivation for the begin of the GFZ activities in GNSS Reflectometry were promising scientific results within the GPS radio occultation experiment of CHAMP (Reigber et al. 2005, Wickert et al. 2001). Specific signatures in the RO data could be clearly assigned to signal reflections from water and ice surfaces (Beyerle et al. 2002). Numerous ground experiments, airborne campaigns or activities to initiate new satellite missions with GNSS-R components by GFZ scientists were performed afterwards (e.g. Cardellach et al. 2018, Wickert et al. 2016, Semmling et al. 2011, 2014). Here we briefly review the main foci of recent GFZ activities in GNSS-R.

### 3.1 Sea ice monitoring

L-band techniques contribute already essentially to sea ice remote sensing. Sea ice thickness, for example, can be estimated with L-band radiometry (e.g., Schmitt and Kaleschke 2018). To fully exploit the potential of GNSS-R for sea ice remote sensing, an improved understanding of the signal reflection in relation to sea ice properties is required. This is the main motivation for our GNSS-R research especially in view to initiate innovative satellite missions (e.g. Cardellach et al. 2018, Wickert et al. 2016).

Related studies were started at GFZ with the GPS sea ice and dry snow (GPS-SIDS) project initiated by the European Space Agency (ESA). An important finding of this project was the significant increase of signal coherence related to sea ice coverage. It results from the change of reflection conditions going from a rough open-water sea surface to a smooth surface at early stages of sea ice formation (Semmling et al. 2011). In addition to the coherence effect, a response of reflected signal power to sea ice ageing was discovered in a 5-month record of the GPS-SIDS project (Fabra et al. 2011). These results led to

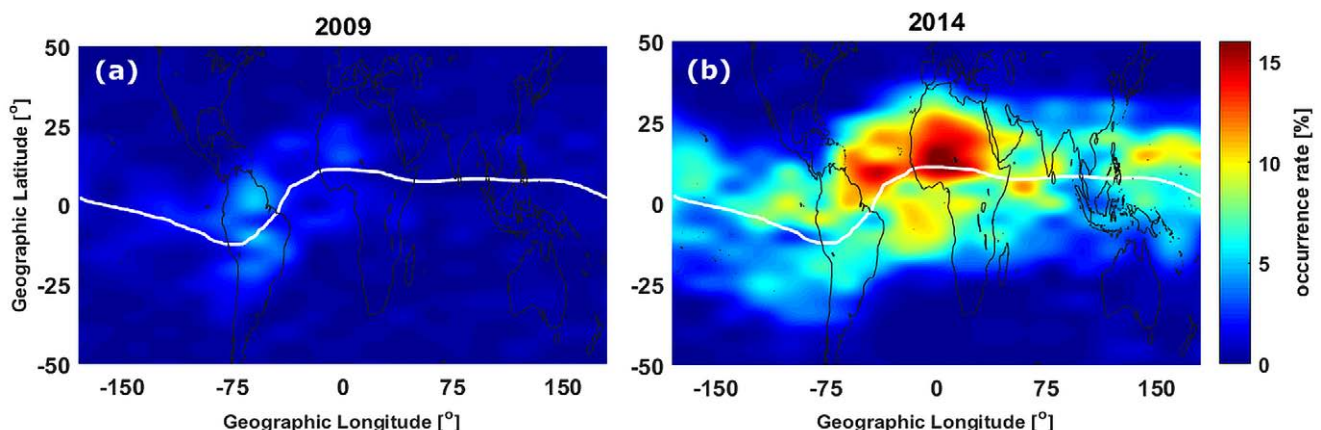


Fig. 14: Global occurrence of EPBs during (a, left) solar minimum year in 2009 and (b, right) solar maximum year in 2014 using GPS radio occultation measurements from FormoSat-3/COSMIC satellites. The occurrence rate is represented within every 20° in longitude by 5° in latitude in the geographic bin. The white solid line depicts the geomagnetic equator.

further investigations using enhanced geodetic GNSS receivers with focus on the signal polarization. An Arctic reflectometry station at Kongsfjorden, Spitsbergen, was established by GFZ in cooperation with the Norwegian Polar Institute (NPI) and the Alfred Wegener Institute (AWI). A long-term data analysis identified reflection signatures of glaciers in the Kongsfjorden area (Peraza et al. 2017). The feasibility of sea ice investigations, there, is affected, however, by the progressive retreat of sea ice over the years.

A new GFZ approach towards GNSS sea ice observations uses ship-based measurements, again in cooperation with NPI and AWI. As a recent result (Fig. 15) sea ice concentration was retrieved during a cruise of the Norwegian research vessel Lance in the Fram Strait (Semmling et al. 2019). Valuable measurements are currently conducted within the MOSAiC expedition in the central Arctic during the drift of the German icebreaker Polarstern, see Fig. 16. Our ship-based approach has the potential to assist navigation in the Arctic. Ships in the Arctic need to report regularly sea ice observations and can benefit from ancillary GNSS measurements.

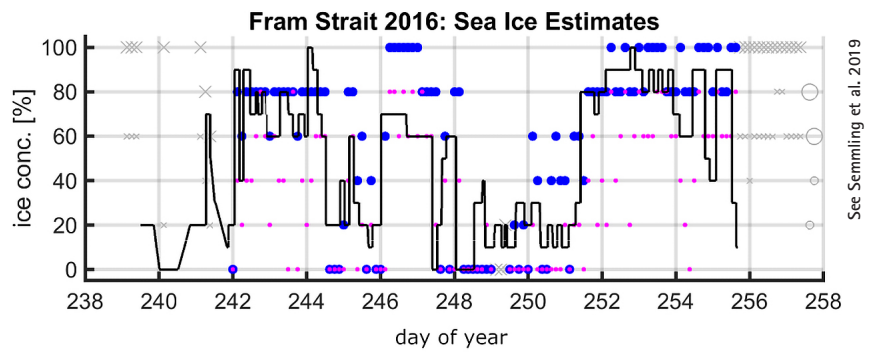


Fig. 15: Sea ice concentration results from the cruise of R/V Lance in the Fram Strait. GNSS-based estimates (blue and magenta dots) are validated against ancillary observations (black line).



Fig. 16: GNSS reflectometry concept for sea ice observations using the GFZ setup aboard R/V Polarstern.

### 3.2 Meteorological applications

The GNSS signal reflection pattern is proportional to the ocean state, which is mainly controlled by the surface wind speed. In this sense, wind speed can be extracted on global scale through analyzing the signals intercepted by cheap and cost-effective GNSS receivers on-board small satellites.

The GFZ algorithm deriving the wind speed from measurements of the British satellite TechDemoSat-1 (TDS-1) was developed to evaluate and characterize the GNSS-R wind speed data (Asgarimehr et al. 2018a). Fig. 17 shows the derived global wind speed using this dataset. The resulting ocean winds are compared to those from the Advanced Scatterometer (ASCAT) as a well-established ocean remote sensing instrument. The GNSS-R-based wind speed data products show comparable quality and more robustness during rain events. Our study demonstrated the accuracy of the GNSS-R technology as

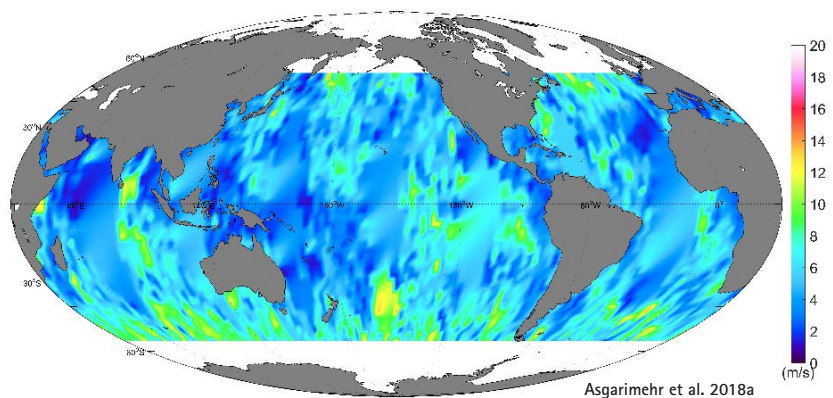
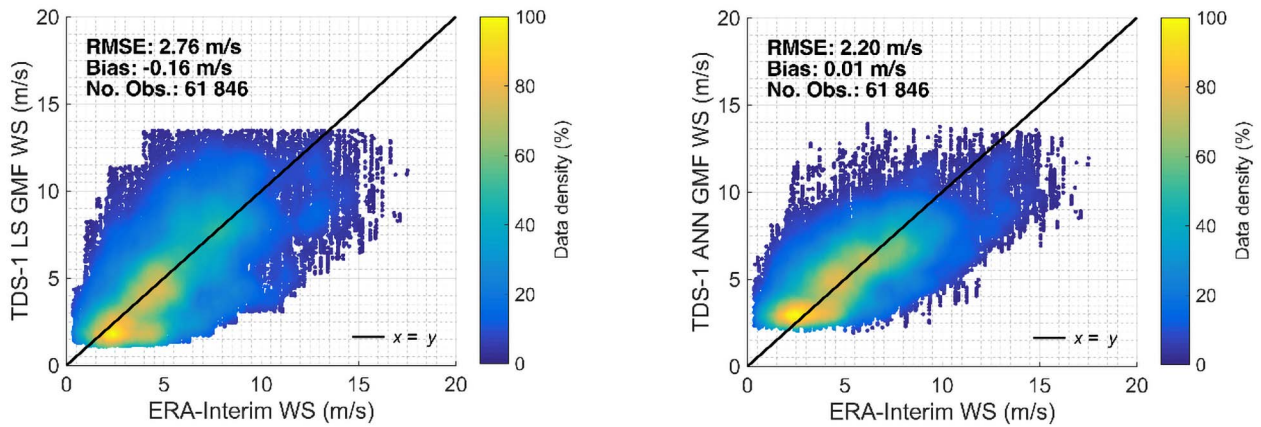


Fig. 17: Average global wind speed using TechDemoSat-1 measurements from May 2015 to June 2016.

well as its excellent suitability during rain events and documented its capability in ocean wind speed monitoring during severe weather.

Modern data scientific approaches could lead to even higher-quality wind speed retrievals. The wind speeds, derived from a machine learning technique compared to



Asgarimehr et al. 2019a.

Fig. 18: Wind speed with a conventional method (left) and using a machine learning algorithm (right) versus ERA-Interim test observations.

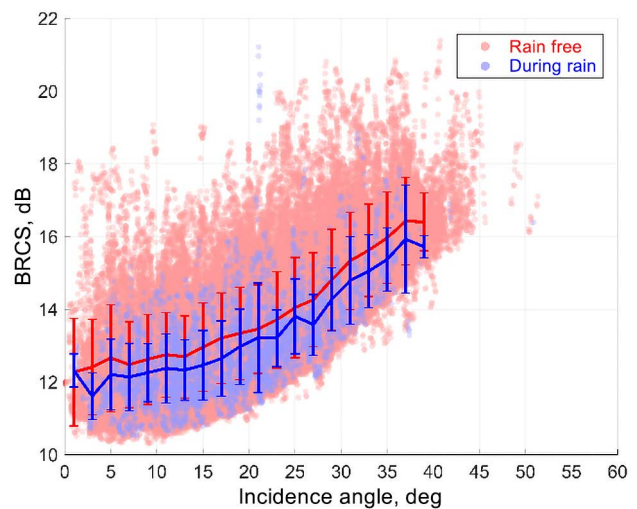
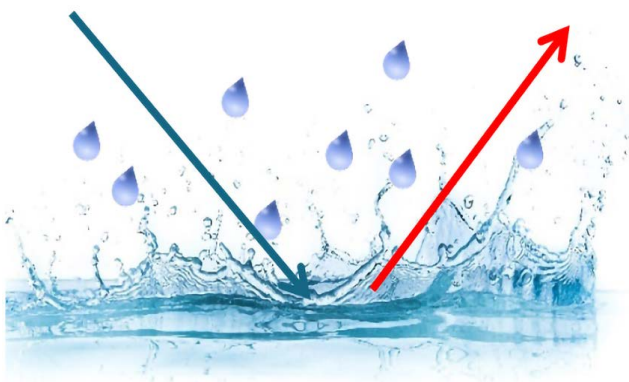
a conventional method, are compared in Fig. 18. The machine learning approach demonstrates an ability to model a variety of effects degrading the retrieval accuracy. This advantageous capability results in higher accuracy of the data products (Asgarimehr et al. 2019a).

GNSS signals have been hardly considered as a rain indicator. This is because the GNSS signals are designed so that their energy is not absorbed by raindrops in the atmosphere. It is further shown that the rain signal attenuation has an insignificant effect on GNSS-R wind speeds (Asgarimehr et al. 2019b). Although the wind data exhibit a high level of robustness during rain events, it is shown that the splash effect is trackable with spaceborne GNSS-R over oceans induced by low to moderate winds. The roughness of the sea surface is altered by raindrops impinging on the ocean surface, as illustrated in Fig. 19 (left). As a result, the measurements can be potentially used for rain detection over calm oceans (Asgarimehr et al. 2018b). The Bistatic Radar Cross Section (BRCS) represents the cross section of ocean facets correctly

oriented to scatter forward the GNSS signals toward the receiver. The modifications in the surface roughness by rain splash causes a reduction in the BRCS value at low wind speed as shown in Fig. 19 (right). This study may have a high impact to introduce an innovative GNSS-R application with potentially new rainfall datasets in the near future.

### 3.3 Soil moisture monitoring

An important GNSS remote sensing application based on the usage of already existing infrastructures is the derivation of land surface parameters in the vicinity of GNSS ground stations. Fig. 20 shows, as example, the temporal variation of soil moisture nearby the GFZ ground station Sutherland, South Africa, in 2014. The analysis is based on the evaluation of the SNR of the GNSS signal, from which the penetration depth into the soil can be derived, which depends on the soil moisture. The GNSS-based



Asgarimehr et al. 2018b.

Fig. 19: Illustration of rain splash (left) and its signature in TDS-1 measurements (right): the bistatic radar cross section versus the reflection incidence angle during rain events (blue) and in rain-free condition (red) at wind speeds between 2 to 4 m/s.

observations reflect very well the precipitation events and subsequent evaporation and agree with the independent observations from in-situ Time Domain Reflectometry (TDR) sensors within 6 Vol % (Vey et al. 2016a). Such observations have the potential to densify the global observing network for soil moisture at many of globally distributed GNSS stations. Snow heights nearby the station can be precisely derived using the same analysis technique (Vey et al. 2016b).

We currently apply this method within the International Research Training Group Strategy, funded by the DFG and the federal state of Brandenburg. The project focuses on monitoring key hydrological parameters, such as IWV and soil moisture, in the Central Andes using modern GNSS remote sensing methods. The region is characterized by severe changes in the climate conditions, which affect various environmental and socio-economic aspects of the area. It has been noted that the local precipitation is tightly connected with the topography and, more specifically, the most intense occurrences take place in the base of the mountains (Bookhagen et al. 2008). Four independent GNSS ground stations and in-situ soil-moisture sensors were installed in the Salta Province, Argentina, in spring 2019 (see Fig. 21). Each station is located at different altitudes and contains various GNSS receivers to investigate the performance of low-cost receivers for soil moisture observations compared to geodetic standard receivers. Additionally, meteorological information is used for studying the correlation between the precipitation events and soil moisture changes as well as the time lag between those events and the changes that occur in the soil humidity. GNSS-based IWV will be used in addition to investigate the relation linking the water content in the atmosphere and the atmospheric conditions that are needed towards triggering a precipitation event.

#### 4 Summary and outlook

GNSS remote sensing applications have developed into a versatile and sound complement of existing Earth observation techniques during the recent years. Thanks to intense and broad research activities, GFZ could actively stimulate these developments. Our contribution briefly reviews current research work with, in part, operational applications. Ground- and satellite-based neutral atmosphere and ionosphere sounding techniques are well developed and acknowledged, main applications are

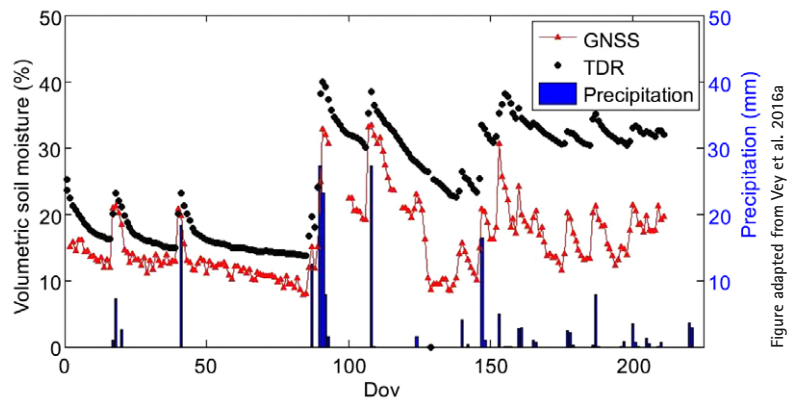


Figure adapted from Vey et al. 2016a

Fig. 20: Soil moisture variation in Sutherland, South Africa, derived from GNSS data (red) and TDR sensors (black). Blue bars indicate precipitation events.



Figure: N. Antonoglou

Fig. 21: GNSS station installed in Payogasta, Salta, Argentina. The station is powered by solar panels and it is equipped with a Novatel SMART-V1G and a Geostar GeoS-5M EVK GNSS receiver.

weather forecast, climate research and space weather. The GNSS Reflectometry exhibits a high potential for various geophysical applications, as weather forecast, part of early warning systems, and climate research. It is currently still in the development phase under active participation of GFZ scientists. The transition from the single GPS to a Multi-GNSS system, extended by GLONASS, Galileo and BeiDou, with extension of related receiver infrastructure, increases accuracy, reliability and operability of the GNSS remote sensing applications with improved spatio-temporal resolution of the observations.

#### Acknowledgements

The solar flux and Ap data (Fig. 8) are provided by the National Research Council of Canada and GFZ Potsdam.

## References

- Arras, C., Wickert, J., Jacobi, C., Heise, S., Beyerle, G., Schmidt, T. (2008): A global climatology of ionospheric irregularities derived from GPS radio occultation. *Geophysical Research Letters*, 35, L14, 809. DOI: 10.1029/2008GL034158.
- Arras, C. (2010): A Global Survey of Sporadic E Layers based on GPS Radio Occultations by CHAMP, GRACE and FORMOSAT-3/COSMIC. STR 10/09, GFZ Potsdam. ISSN1610-0956.
- Asgarimehr, M., Zhelavskaya, I., Foti, G., Reich, S., Wickert, J. (2019a): A GNSS-R Geophysical Model Function: Machine Learning for Wind Speed Retrievals. *IEEE Geoscience and Remote Sensing Letters*. Accepted for publication.
- Asgarimehr, M., Wickert, J., Reich, S. (2019b): Evaluating Impact of Rain Attenuation on Space-borne GNSS Reflectometry Wind Speeds. *Remote Sensing*, 11, 9, 1048.
- Asgarimehr, M., Wickert, J., Reich, S. (2018a): TDS-1 GNSS Reflectometry: Development and Validation of Forward Scattering Winds. *IEEE Journal of Selected Topics in Applied Earth Observations and Remote Sensing*, 11, 11, 4534–4541.
- Asgarimehr, M., Zavorotny, V., Wickert, J., Reich, S. (2018b): Can GNSS reflectometry detect precipitation over oceans? *Geophysical Research Letters*, 45, 22, 12-585.
- Bender, M., Dick, G., Ge, M., Deng, Z., Wickert, J., Kahle, H.-G., Raabe, A., Tetzlaff, G. (2011): Development of a GNSS water vapor tomography system using algebraic reconstruction techniques. *Advances in Space Research*, 47, 10, 1704–1720.
- Beyerle, G., Hocke, K., Wickert, J., Schmidt, T., Marquardt, C., Reigber, C. (2002): GPS radio occultations with CHAMP: A radio holographic analysis of GPS signal propagation in the troposphere and surface reflections. *Journal of Geophysical Research*, 107, D24. DOI: 10.1029/2001JD001402.
- Bookhagen, B., Strecker, M.R. (2008): Orographic barriers, high-resolution TRMM rainfall, and relief variations along the eastern Andes. *Geophysical Research Letters*, 35, 6.
- Cardellach, E., Wickert, J., Baggen, R., Benito, J., Camps, A., Catarino, N., Chapron, B., Dielacher, A., Fabra, F., Flato, G., Fragner, H., Gabarró, C., Gommenginger, C., Haas, C., Healy, S., Hernandez-Pajares, M., Høeg, P., Jäggi, A., Kainulainen, J., Khan, S.A., Lemke, N.M., Li, W., Nghiem, S.V., Pierdicca, N., Portabella, M., Rautiainen, K., Rius, A., Sasgen, I., Semmling, M., Shum, C., Soulat, F., Steiner, A.K., Tailhades, S., Thomas, M., Vilaseca, R., Zuffada, C. (2018): GNSS Transpolar Earth Reflectometry explorINg system (G-TERN): Mission concept. *IEEE Access*, 6, 13980–14018. DOI: 10.1109/ACCESS.2018.2814072.
- Cardinali, C., Healy, S. (2014): Impact of GPS radio occultation measurements in the ECMWF system using adjoint-based diagnostics. *Q.J.R. Meteorol. Soc.* 140: 2315–2320. DOI: 10.1002/qj.2300.
- Dick, G., Gendt, G., Reigber, C. (2001): First Experience with Near Real-Time Water Vapor Estimation in a German GPS Network. *Journal of Atmospheric and Solar-Terrestrial Physics*, 63, 1295–1304.
- Elgered, G., Wickert, J. (2017): Monitoring of the Neutral Atmosphere. In: Teunissen, P.J.G., Montenbruck, O. (Eds.): *Springer Handbook of Global Navigation Satellite Systems*, (Springer Handbooks), Berlin [u.a.], 1109–1138. DOI: 10.1007/978-3-319-42928-1\_38.
- Fabra, F., Cardellach, E., Rius, A., Ribó, S., Oliveras, S., Belmonte, M., Semmling, M., D'Addio, M.S. (2011): Phase Altimetry with Dual Polarization GNSS-R over Sea Ice. *IEEE Geosci. Remote Sens.*, 50, 2112–2121.
- Ge, M., Gendt, G., Dick, G., Zhang, F. (2005): Improving the carrier phase ambiguity resolution in global GPS network solution. *Journal of Geodesy*, 79, 103–110. DOI: 10.1007/s00290-005-0447-0.
- Gendt, G., Dick, G., Reigber, C., Tomassini, M., Liu, Y., Ramatschi, M. (2004): Near real time GPS water vapor monitoring for numerical weather prediction in Germany. *J. Met. Soc. Japan*, 82(1B), 361–370.
- Hall, C.D., Cordey, R.A. (1988): Multistatic scatterometry, International Geoscience and Remote Sensing Symposium. *Remote Sensing: Moving Toward the 21st Century*, Vol. 1, 561–562, IEEE.
- Hernández-Pajares, M., Juan, J.M., Sanz, J., Orus, R., Garcia-Rigo, A., Feltens, J., Komjathy, A., Schaer, S.C., Krankowski, A. (2009): The IGS VTEC maps: a reliable source of ionospheric information since 1998. *Journal of Geodesy*, 83(3–4), 263–275.
- Hernández-Pajares, M., Juan, J.M., Sanz, J. (2006): Medium-scale traveling ionospheric disturbances affecting GPS measurements: Spatial and temporal analysis. *J. Geophys. Res.*, 111, A07S11. DOI: 10.1029/2005JA011474.
- Jakowski, N. (2007): Ionosphere Monitoring, In: Teunissen, P.J.G., Montenbruck, O. (Eds.): *Springer Handbook of Global Navigation Satellite Systems*, (Springer Handbooks), Berlin [u.a.], 1139–1162. DOI: 10.1007/978-3-319-42928-1\_38.
- Jonah, O.F., Kherani, E.A., De-Paula, E.R. (2016): Observation of TEC perturbation associated with medium-scale traveling ionospheric disturbance and possible seeding mechanism of atmospheric gravity wave at a Brazilian sector. *J. Geophys. Res. Space Physics*, 121, 2531–2546. DOI: 10.1002/2015JA022273.
- Kačmařík, M., Douša, J., Zus, F., Václavovic, P., Balidakis, K., Dick, G., Wickert, J. (2019): Sensitivity of GNSS tropospheric gradients to processing options. *Ann. Geophys.*, 37, 429–446.
- Katzberg, S., Garrison, J. (December 1996): Utilizing GPS to Determine Ionospheric Delay Over the Ocean. NASA TM 4750.
- Kepkar, A., Arras, C., Wickert, J., Schuh, H., Alizadeh, M., Tsai, L.C. (2020): Occurrence climatology of equatorial plasma bubbles derived using FormoSat-3/COSMIC GPS radio occultation data. *Ann. Geophys.*, 38, 611–623. DOI: 10.5194/angeo-38-611-2020.
- Li, X., Zus, F., Lu, C., Ning, T., Dick, G., Ge, M., Wickert, J., Schuh, H. (2015b): Retrieving high resolution tropospheric gradients from multi-constellation GNSS observations. *Geophys. Res. Lett.*, 42, 4173–4181. DOI: 10.1002/2015GL063856.
- Martin-Neira, M. (1993): A passive reflectometry and interferometry system PARIS: Application to ocean altimetry. *ESA Journal*, 17, 331–355.
- Ning, T., Wickert, J., Deng, Z., Heise, S., Dick, G., Vey, S., Schöne, T. (2016a): Homogenized time series of the atmospheric water vapor content obtained from the GNSS reprocessed data. *Journal of Climate*, 29, 7, 2443–2456. DOI: 10.1175/JCLI-D-15-0158.1.
- Ning, T., Wang, J., Elgered, G., Dick, G., Wickert, J., Bradke, M., Sommer, M. (2016b): The uncertainty of the atmospheric integrated water vapour estimated from GNSS observations. *Atmospheric Measurement Techniques*, 9, 79–92. DOI: 10.5194/amt-9-79-2016.
- Peraza, L., Semmling, A.M., Falck, C., Pavlova, O., Gerland, S., Wickert, J. (2017): Analysis of Grazing GNSS Reflections Observed at the Zeppelin Mountain Station. *Spitsbergen, Radio Science*, 52, 1352–1362.
- Petit, G., Luzum, B. (Eds.) (2010): *IERS Conventions (2010)*, IERS Technical Note, 36, Frankfurt am Main, Verlag des Bundesamts für Kartographie und Geodäsie, 179 pp., ISBN 3-89888-989-6.
- Pi, X., Mannucci, A.J., Lindqwister, U.J., Ho, C.M. (1997): Monitoring of global ionospheric irregularities using the worldwide GPS networks. *Geophys. Res. Lett.*, 24 (18), 2283–2286. DOI: 10.1029/97GL02273.
- Ramatschi, M., Bradke, M., Nischan, T., Männel, B. (2019): GNSS data of the global GFZ tracking network. Data publication. DOI: 10.5880/GFZ.1.1.2020.001.
- Reigber, C., Lühr, H., Schwintzer, P., Wickert, J. (Eds.) (2005): *Earth Observation with CHAMP: Results from Three Years in Orbit*. Springer Berlin Heidelberg New York, ISBN 3-540-22804-7.
- Reigber, C., Gendt, G., Wickert, J. (2004): GPS Atmosphären-Sondierungs-Projekt (GASP): Ein innovativer Ansatz zur Bestimmung von Atmosphärenparametern. Scientific Technical Report GFZ STR 04/02.
- Rinke, A., Segger, B., Crewell, S., Maturilli, M., Naakka, T., Nygård, T., Vihma, T., Alshawaf, F., Dick, G., Wickert, J., Keller, J. (2019): Trends of Vertically Integrated Water Vapor over the Arctic during 1979–2016: Consistent Moistening All Over? *Journal of Climate*, 32, 18, 6097–6116. DOI: 10.1175/JCLI-D-19-0092.1.
- Rius, A., Cardellach, E. (2017): Reflectometry. In: Teunissen, P.J.G., Montenbruck, O. (Eds.): *Springer Handbook of Global Navigation Satellite Systems*, (Springer Handbooks), 1163–1186. DOI: 10.1007/978-3-319-42928-1\_38.
- Schmidt, T., Alexander, P., de la Torre, A. (2016): Stratospheric gravity wave momentum flux from radio occultations. *J. Geophys. Res. Atmos.*, 121. DOI: 10.1002/2015JD024135.
- Schmidt, T., Wickert, J., Haser, A. (2010): Variability of the upper troposphere and lower stratosphere observed with GPS radio occultation bending angles and temperatures. *Adv. Space Res.*, 46(2), 150–161. DOI: 10.1016/j.asr.2010.01.021.

- Schmidt, T., Wickert, J., Beyerle, G., König, R., Galas, R., Reigber, C. (2005): The CHAMP atmospheric processing system for radio occultation measurements. In: Reigber C., Lühr, H., Schwintzer, P., Wickert, J. (Eds): Earth Observation with CHAMP. Springer, Berlin, ISBN 3-540-22804-7, 597–602.
- Schmitt, A. U., Kaleschke, L. (2018): Consistent Combination of Brightness Temperatures from SMOS and SMAP over Polar Oceans for Sea Ice Applications. *Remote Sens.*, 10.
- Semmling, A. M., Rösel, A., Divine, D., Gerland, S., Stienne, G., Reboul, S., Ludwig, M., Wickert, J., Schuh, H. (2019): Sea Ice concentration derived from GNSS reflection measurements in Fram Strait. *IEEE Trans. Geosci. Remote Sens.*, 57, 10350–10361.
- Semmling, A. M., Beckheinrich, J., Wickert, J., Beyerle, G., Schön, S., Fabra, F., Pflug, H., He, K., Schwabe, J., Scheinert, M. (2014): Sea surface topography retrieved from GNSS-R phase data of the GEOHALO flight mission. *Geophys. Res. Lett.* 41, 3, 954–960. DOI: 10.1002/2013GL058725.
- Semmling, A. M., Beyerle, G., Stosius, R., Dick, G., Wickert, J., Fabra, F., Cardellach, E., Ribo, S., Rius, A., Helm, A., Yudanov, S., d'Addio, S. (2011): Detection of Arctic Ocean tides using interferometric GNSS-R signals. *Geophys. Res. Lett.*, 38, L04103. DOI: 10.1029/2010GL046005.
- Skamarock, W. C., Klemp, J. B., Dudhia, J., Gill, D. O., Barker, D. M., Duda, M. G., Huang, X. Y., Wang, W., and Powers, J. G. (2008): A Description of the Advanced Research WRF Version 3, NCAR Tech. Note NCAR/TN-475+STR, NCAR: Boulder, CO, USA.
- Steiner, A. K., Ladstädter, F., Ao, C. O., Gleisner, H., Ho, S.-P., Hunt, D., Schmidt, T., Foelsche, U., Kirchengast, G., Kuo, Y.-H., Lauritsen, K. B., Mannucci, A. J., Nielsen, J. K., Schreiner, W., Schwärz, M., Sokolovskiy, S., Syndergaard, S., Wickert, J. (2020): Consistency and structural uncertainty of multi-mission GPS radio occultation records. *Atmos. Meas. Tech.*, 13, 2547–2575.
- Stosius, R., Beyerle, G., Hoehner, A., Wickert, J., Lauterjung, J. (2011): The impact on tsunami detection from space using GNSS-reflectometry when combining GPS with GLONASS and Galileo on GNSS-Reflectometry tsunami detection from space. *Advances in Space Research*, 47, 5, 843–853.
- Vey, S., Güntner, A., Wickert, J., Blume, T., Ramatschi, M. (2016a): Long-term soil moisture dynamics derived from GNSS interferometric reflectometry: a case study for Sutherland, South Africa. *GPS Solutions*, 20, 4, 641–654. DOI: 10.1007/s10291-015-0474-0.
- Vey, S., Güntner, A., Wickert, J., Blume, T., Thoss, H., Ramatschi, M. (2016b): Monitoring Snow Depth by GNSS Reflectometry in Built-up Areas: A Case Study for Wettzell, Germany. *IEEE Journal of selected topics in applied earth observations and remote sensing*, Vol. 9, Issue: 10, 4809–4816. DOI: 10.1109/JSTARS.2016.2516041.
- Wickert, J., Cardellach, E., Martín-Neira, M., Bandejas, J., Bertino, L., Andersen, O. B., Camps, A., Catarino, N., Chapron, B., Fabra, F., Floury, N., Foti, G., Gommenginger, C., Hatton, J., Høeg, P., Jäggi, A., Kern, M., Lee, T., Li, Z., Park, H., Pierdicca, N., Ressler, G., Rius, A., Roselló, J., Saynisch, J., Soulat, F., Shum, C. K., Semmling, M., Sousa, A., Xi, J., Zuffada, C. (2016): GEROS-ISS: GNSS Reflectometry, Radio Occultation, and Scatterometry Onboard the International Space Station. *IEEE Journal of Selected Topics in Applied Earth Observations and Remote Sensing*, 9, 10, 4552–4581. DOI: 10.1109/JSTARS.2016.2614428.
- Wickert, J., Michalak, G., Schmidt, T., Beyerle, G., Cheng, C. Z., Healy, S. B., Heise, S., Huang, C. Y., Jakowski, N., Köhler, W., Mayer, C., Offiler, D., Ozawa, E., Pavelyev, A. G., Rothacher, M., Tapley, B., Arras, C. (2009): GPS radio occultation: results from CHAMP, GRACE and FORMOSAT-3/COSMIC. *Terrestrial Atmospheric and Oceanic Sciences*, 20, 1, 35–50.
- Wickert, J., Pavelyev, A., Liou, Y., Schmidt, T., Reigber, C., Igarashi, K., Pavelyev, A., and Matyugov, S. (2004): Amplitude variations in GPS signals as a possible indicator of ionospheric structures. *Geophys. Res. Lett.*, 31, L24 801. DOI: 10.1029/2004GL020607.
- Wickert, J., Reigber, C., Beyerle, G., König, R., Schmidt, T., Grunwaldt, L., Galas, R., Meehan, T., Melbourne, W. G., Hocke, K. (2001): Atmosphere sounding by GPS radio occultation: First Results from CHAMP. *Geophysical Research Letters*, 28, 17, 3263–3266.
- Zavorotny, V. U., Gleason, S., Cardellach E., Camps, A. (2014): Tutorial on remote sensing using GNSS bistatic radar of opportunity. *IEEE Geoscience and Remote Sensing Magazine* 2, 8–45.
- Zus, F., Douša, J., Kačmařík, M., Václavovic, P., Dick, G., Wickert, J. (2019a): Estimating the Impact of Global Navigation Satellite System Horizontal Delay Gradients in Variational Data Assimilation. *Remote Sens.*, 11, 41.
- Zus, F., Douša, J., Kačmařík, M., Václavovic, P., Balidakis, K., Dick, G., Wickert, J. (2019b): Improving GNSS Zenith Wet Delay Interpolation by Utilizing Tropospheric Gradients: Experiments with a Dense Station Network in Central Europe in the Warm Season. *Remote Sens.*, 11, 674.
- Zus, F., Dick, G., Douša, J., Heise, S., Wickert, J. (2014): The rapid and precise computation of GPS slant total delays and mapping factors utilizing a numerical weather model. *Radio Sci.*, 49, 207–216.

Contact

Prof. Dr. Jens Wickert | Prof. Dr. Maorong Ge | Prof. Dr. Harald Schuh | Dr. Karina Wilgan | Ankur Kepkar | Chinh Nguyen | Temitope Seun Oluwadare  
 German Research Centre for Geosciences GFZ  
 Telegrafenberg, 14473 Potsdam, Germany  
 also at  
 Technische Universität Berlin  
 Straße des 17. Juni 135, 10623 Berlin, Germany  
 wickert@gfz-potsdam.de | maor@gfz-potsdam.de | schuh@gfz-potsdam.de | wilgan@gfz-potsdam.de | kepkar@gfz-potsdam.de | chnh@gfz-potsdam.de | oluwa@gfz-potsdam.de

Dr. Galina Dick | Dr. Torsten Schmidt | Dr. Milad Asgarimehr | Dr. Christina Arras | Dr. Andreas Brack | Dr. Benjamin Männel | Dr. Sibylle Vey | Dr. Florian Zus  
 German Research Centre for Geosciences GFZ  
 Telegrafenberg, 14473 Potsdam, Germany  
 dick@gfz-potsdam.de | tschmidt@gfz-potsdam.de | milad@gfz-potsdam.de | arras@gfz-potsdam.de | andreas.brack@gfz-potsdam.de | benjamin.maennel@gfz-potsdam.de | vey@gfz-potsdam.de | zusflo@gfz-potsdam.de

Nikolaos Antonoglou  
 Universität Potsdam  
 Karl-Liebknecht-Straße 24-25, 14476 Potsdam-Golm, Germany  
 also at  
 German Research Centre for Geosciences GFZ  
 Telegrafenberg, 14473 Potsdam, Germany  
 antonogl@gfz-potsdam.de

Dr. Maximilian Semmling  
 German Aerospace Center, Institute for Solar-Terrestrial Physics  
 Kalkhorstweg 53, 17235 Neustrelitz, Germany  
 maximilian.semmling@dlr.de

Tzvetan Simeonov  
 Deutscher Wetterdienst, Meteorologisches Observatorium Lindenberg  
 15848 Tauche, Germany  
 tzvetan.simeonov@dwd.de

This article also is digitally available under [www.geodaesie.info](http://www.geodaesie.info).